Accelerated Pavement Testing of Geocell-reinforced Bases over Weak Subgrade

Sanat Kumar Pokharel, Ph.D. candidate
Civil, Environmental, and Architectural Engineering Department, the University of Kansas, 1530 W. 15th street, Lawrence, KS 66045-7609.
Phone: 785-864-2923, Email: sanpok@ku.edu

Jie Han*, Ph.D., P.E.
Associate Professor, Civil, Environmental, and Architectural Engineering Department, the University of Kansas, 1530 W. 15th street, Lawrence, KS 66045-7609.
Phone: 785-864-3714, Email: jiehan@ku.edu

Chandra Manandhar, Ph.D. candidate
Department of Civil Engineering, Kansas State University, Manhattan, Kansas,
Phone: 785-317-9132, Email: cmanandh@k-state.edu

Xiaoming Yang, Ph.D. candidate
Civil, Environmental, and Architectural Engineering Department, the University of Kansas, 1530 W. 15th street, Lawrence, KS 66045-7609.

Dov Leshchinsky, Ph.D.
Professor, Department of Civil and Environmental Engineering, the University of Delaware, Newark, DE19719. Email: reslope@aol.com

Izhar Halahmi
Chief Scientist, PRS Mediterranean Ltd.
2 Weizmann St., Tel-Aviv 64239, Israel
Email: izharhal@012.net.il

Robert L. Parsons, Ph.D., P.E.
Associate Professor, Civil, Environmental, and Architectural Engineering Department, the University of Kansas, 1530 W. 15th street, Lawrence, KS 66045-7609.
Phone: 785-864-2946, Email: rparsons@ku.edu

Word Count: 7379
Number of words in text: 4129
Number of Figures: 13

* the corresponding author

March 31, 2010

Abstract: To evaluate the effect of geocell reinforcement on base courses for low-volume unpaved roads over weak subgrade, full-scale trafficking tests were conduced using the accelerated pavement testing facility at Kansas State University. Three different types of infill materials including AB3 aggregate, quarry waste (QW), and Recycled Asphalt Pavement (RAP) were used for the base courses and A-7-6 clay was used as the subgrade. Four unpaved sections that included one unreinforced control section of 30 cm thick AB3 aggregate and other three 15 cm polymeric alloy geocell-reinforced sections with 2cm cover were tested under the single-axle dual tire wheel loading. The benefits of alloy geocell reinforcement are evaluated in terms of rut depths at a number of passes of the wheel load and the angle of stress distribution from the surface to the base course-subgrade interface. The test results demonstrated that the alloy geocell reinforcement improved the performance of unpaved AB3 and RAP sections in terms of rut depth and angle of stress distribution compared to the unreinforced section. The QW section also showed better performance in terms of stress distribution angle. The road sections were exhumed and evaluated after the moving wheel test.

Keywords: Geocell, low-volume roads, unpaved roads, accelerated pavement testing.

INTRODUCTION

Nearly 80% of the roads in the world are low-volume unpaved roads (*1*). In low-volume roads structural strength of the base course and the stress transmitted to the subgrade are two vital factors. Geosynthetics have been successfully used to improve subgrade and reinforce base courses for both unpaved and paved roads for over 40 years (*2*)(3). Geocells, the three-dimensional form of interconnected honeycomb polymeric geosynthetic cells, are used for soil confinement to provide structural strength to the base course. The idea of cellular lateral confinement was first developed and tested by the United States Army Corps of Engineers in 1970s to improve the bearing capacity of poorly-graded sand (*4*). Geocells come in different shapes and sizes with variations in the type of material used, the aspect ratio, and the height and thickness of the cells, however, the most common shape of geocell is near circular layout. Most of the commercially available geocells are made of high-density polyethylene (HDPE). However, some new geocells are currently available, made of stiffer and more creep resistant polymeric alloys.

Lateral confinement, beam (tension membrane) effect, and load distribution at a wider angle are the major geocell reinforcement mechanisms. The geocell-reinforced bases exhibit bending resistance, tensile strength, and shear strength and intercept the failure planes from the subgrade (*5*). The mechanism by which the granular material responds to the repeated traffic loading dictates the design of pavements. The three-dimensional structure of geocell provides the vertical confinement by the friction between the infill material and the geocell wall and the action of the geocell-reinforced base as a mattress to restrain the soil from moving upward outside the loading area.

The beam effect can be evidenced as the tension developed in the curved geocell-reinforced mattress to resist the vertical load (*5*)(*6*)(*7*). As the geocell is stiffer than the surrounding soil, the curved surface exerts upward reaction and reduces the net stress applied to the subgrade. However, to mobilize the beam effect the road section must deform significantly (*2*).

The geocell-reinforced bases can distribute the applied loads to a wider area compared to the unreinforced base (*8*) and a higher bearing capacity can be achieved with a smaller thickness of geocell-reinforced base (*9*). The inclusion of the geocell and the confinement effect thereof would increase the stiffness of the reinforced base. The wider stress distribution caused by geocell reinforcement reduces the stress at the subgrade and increases the bearing capacity. Confinement to limit lateral displacement, formation of stiff mattress for wider load distribution, and contribution of tensile strength to soils are the reported key benefits of geocells.

However, most studies on geocell reinforcement for low-volume roads so far have been based on small-scale or large-scale box tests under static or cyclic loading. Limited studies have been done on geocell-reinforced bases under traffic loading. In this study, geocell-reinforced bases for low-volume unpaved roads were tested under traffic loading in the accelerated pavement testing (APT) facility at Kansas State University.

This paper documents the research work completed by the authors to evaluate the performance of the geocell-reinforced bases over weak subgrade using the APT facility. The major objective of this research was to evaluate the effectiveness of geocells as reinforcement to granular base courses over weak subgrade. This study also assessed the effect of type and quality of base course materials on the performance of geocell-reinforced unpaved roads. To establish the equivalency of geocell-reinforced bases to an unreinforced base, three 17 cm

geocell-reinforced bases with different infill materials and one 30 cm unreinforced base were tested. The infill materials included well-graded aggregate (AB3), quarry waste (QW), and recycled asphalt pavement (RAP). The unreinforced base consisted of well-graded aggregate (AB3). Before the full-scale accelerated moving wheel testing, a series of laboratory tests with single and multiple geocell reinforcement in a medium-size test box were performed under static or cyclic loading. The results of these tests can be found in Pokharel et al. (*10*)(*11*)(*12*)(*13*) and Han et al.(*14*).

FACILITY, EQUIPMENT, AND TEST PREPARATION

Test facilities at the University of Kansas (KU) and Kansas State University (KSU) were used for this research. The material properties were determined at KU while the moving wheel test was carried out at the APT facility of KSU. The material tests included sieve analysis, standard Proctor compaction, and California Bearing Ratio (CBR) tests.

The APT machine has a 12.8 m long reaction frame and a full-scale, 80 kN single axle with dual tires. The dual-wheel axle assemblies are belt-driven using a 20 HP electric motor and a variable frequency drive controls wheel motion. The test pit of the APT facility is 6.1 m long, 4.9 m wide, and 1.8 m deep. The tire pressure used in this study was 552 kPa. The frequency of wheel moving was 0.167 Hz (i.e., 6 sec/pass) and the wheels were run at a speed of 11.3 km/hr within the test pit. In this test, the test pit was divided into four sections of equal dimensions in plan, each section having a length of 3.05 m and a width of 2.45 m. Subgrade was made of A-7-6 soil and prepared to simulate a field condition of CBR value at about 3%. A non-woven geotextile was placed at the subgrade-base interface as a separator. Well-graded aggregate (AB3), quarry waste (QW), and recycled asphalt pavement (RAP) were used as the infill base materials for geocells. The geocells used in this test were NEOLOY™ polymeric alloy (a nano-composite alloy of polyester/polyamide nano-fibers, dispersed in polyethylene matrix) with a cell height of 15 cm. The geocell was laid out in a near circular shape with a dimension of 25 cm in the wheel direction (also the seam direction) and 21 cm in the transverse direction and covered by 2 cm fill. The properties of these materials will be discussed later in this paper. AB3 was also used as the base course for the unreinforced base at a thickness of 30 cm.

MATERIAL PROPERTIES

Geocell and Geotextile

Geocell made of novel polymeric alloy (a nano-composite alloy of polyester/polyamide nano-fibers, dispersed in polyethylene matrix) was used in this study. The novel polymeric alloy is characterized by flexibility at low temperatures similar to HDPE with elastic behavior similar to engineering thermoplastic. Major improvement over old generation HDPE geocells are better creep resistance and better retention of stiffness and creep resistance at elevated temperatures. The geocell used in this study were 15 cm high and had a tensile strength of 19.1 MPa (27.7 KN/m) and an secant elastic modulus of 355 MPa at 2% strain. The tensile stress-strain curve of the geocell is shown in FIGURE 1. The stress-strain curve was measured at a strain rate of 10%/minute at 23^{o} Celsius. The geocell had a wall thickness of 1.1 mm and two perforations of 3.5 cm^{2} each on each pallets of the geocell. A 3.5 oz (99.65 g) non-woven geotextile was used between the subgrade and the base course as a separator in case of reinforced sections.

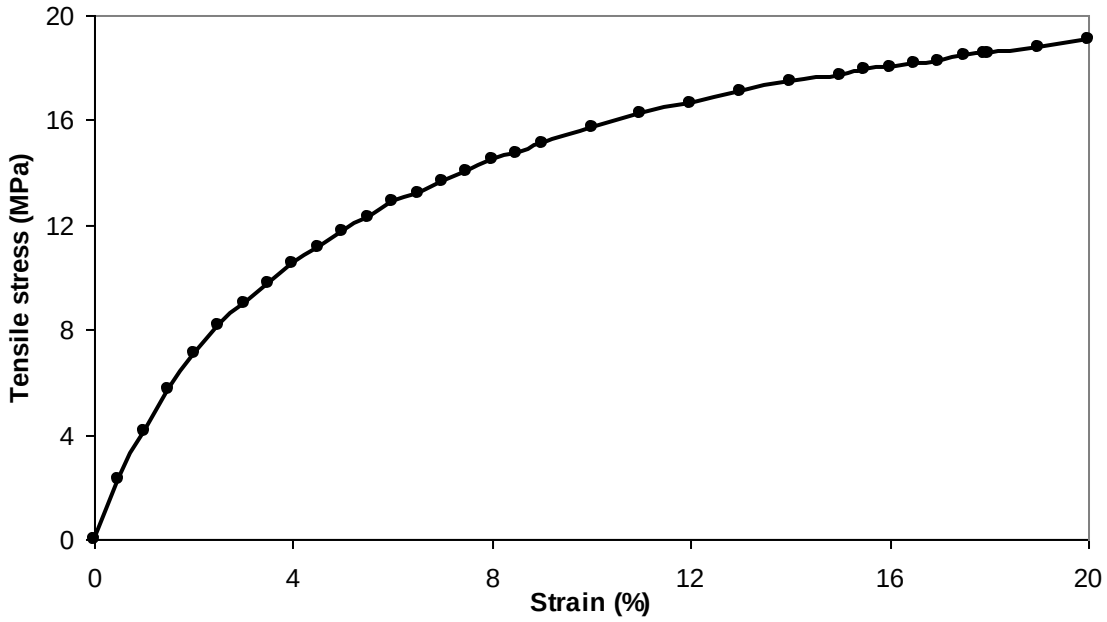

FIGURE 1 Tensile stress-strain curve of the geocell.

Subgrade

A-7-6 clay, locally known as Keats Pit clay in Manhattan area of Kansas, was used as subgrade. Standard Proctor compaction and CBR tests were carried out at the laboratory for this subgrade. An optimum moisture content of 21% and the maximum dry density of 1.61 g/cm^3 were found at the optimum moisture content. The compaction curve and the CBR value at different moisture contents obtained from the laboratory test on the subgrade soil are given in FIGURE 2. A CBR of 3% was achieved at approximately 26% moisture content in the lab, however, it was achieved at approximately 21% in the test pit..

Base course

AB3, QW, and RAP were used as the infill materials for geocells in this study. AB3 was a well-graded base material widely used in low-volume road applications in Kansas, which had a mean particle size (d_{50}) = 4.4 mm, a coefficient of curvature = 1.55, and a coefficient of uniformity = 21. The grain-size distribution of AB3 is shown in FIGURE 4. FIGURES 5 and 6 show the compaction and CBR curves of AB3. Standard Proctor tests indicated that AB3 had an optimum moisture content of 10.2% and a maximum dry density of 2.13 g/cm^3. AB3 had a CBR value of 56% at 9.6% moisture content and 45% at the optimum moisture content, respectively.

QW is a waste material produced during aggregate production in quarries. The QW used in the study was brought from a local quarry site in Kansas. QW had a mean particle size (d_{50}) = 1.3 mm, a coefficient of curvature = 2.3, a coefficient of uniformity = 24, an optimum moisture content = 11%, and a maximum dry density = 2.06 g/cm^3. The grain-size distribution of QW is shown in FIGURE 3. FIGURE 4 shows the compaction and CBR curves for QW. The CBR values of QW were 48% at 8.8% moisture content and 19% at the optimum moisture content, respectively.

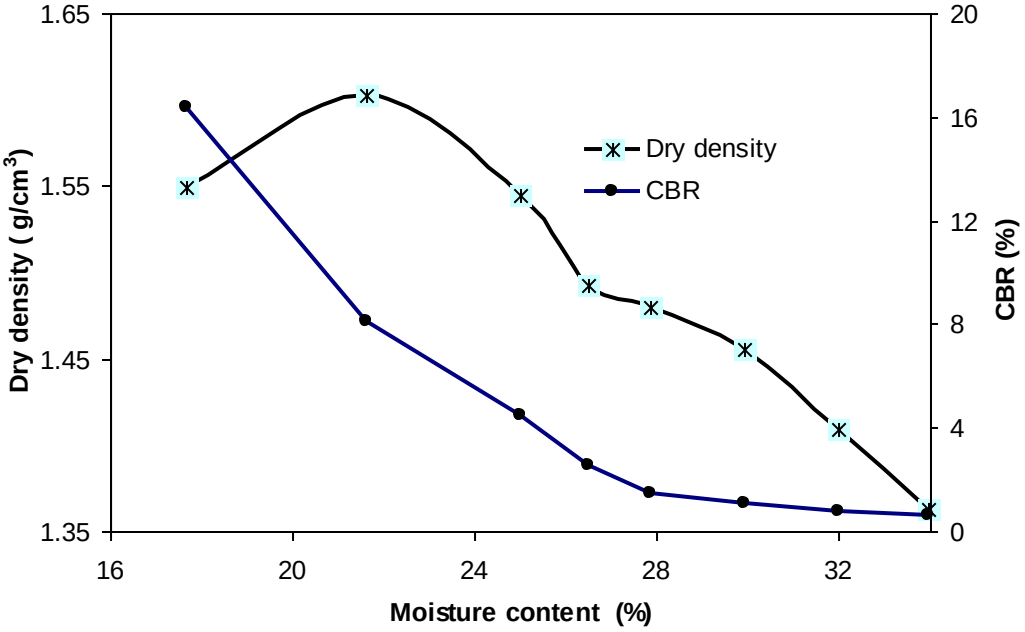

FIGURE 2 Compaction curve and CBR value of subgrade soil.

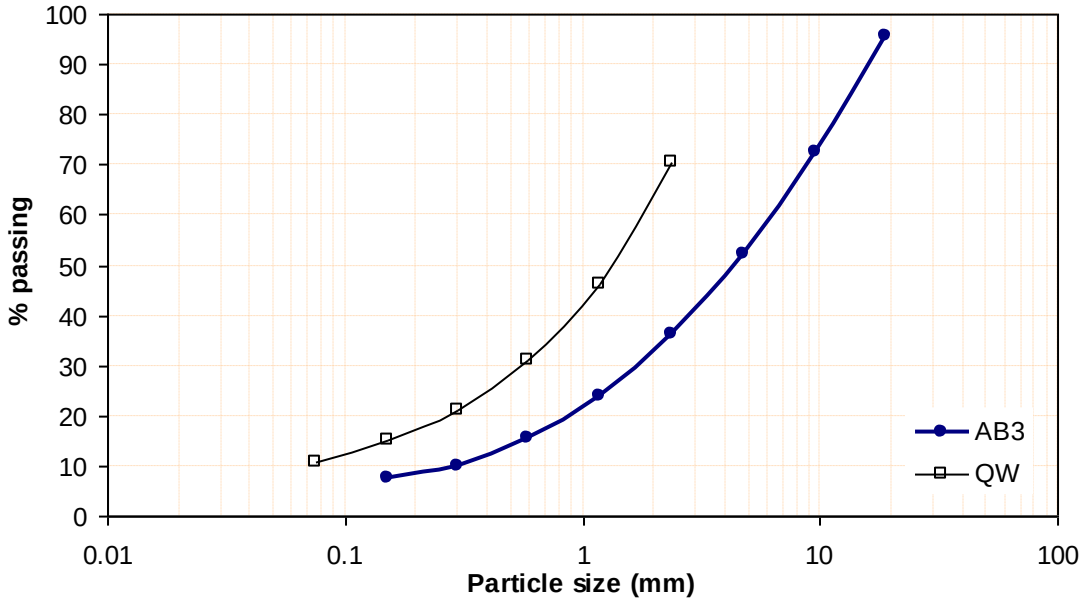

FIGURE 3 Particle size distributions of AB3 and QW.

RAP used in this study was brought from a local RAP supplier in Manhattan, Kansas. The RAP had 5 cm maximum size with a coarse gradation and was sieved through a screen of 5 cm opening size before being placed as the base course. The binder content in the RAP was 6.52%, determined by the ignition method. The compaction and CBR curves for this RAP are shown in FIGURE 5. Test results showed that this RAP had an optimum moisture content of 6%, a maximum dry density of 1.81 g/cm^3, and a CBR value of 10% at 5% moisture content and 8% at the optimum moisture content.

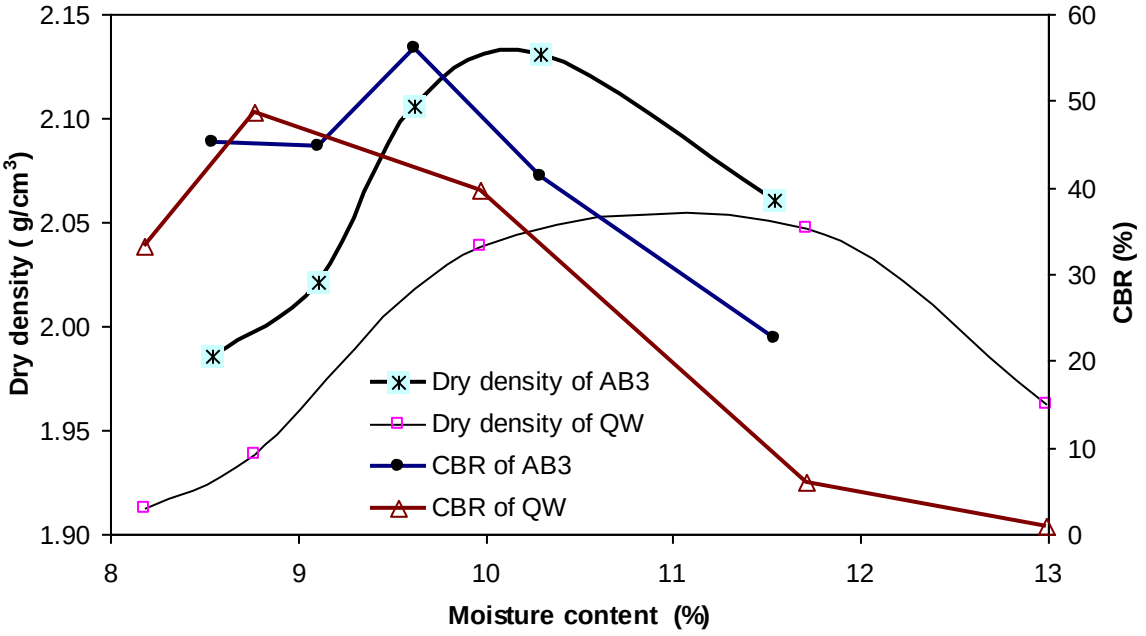

FIGURE 4 Compaction curves and CBR values of AB3 and QW.

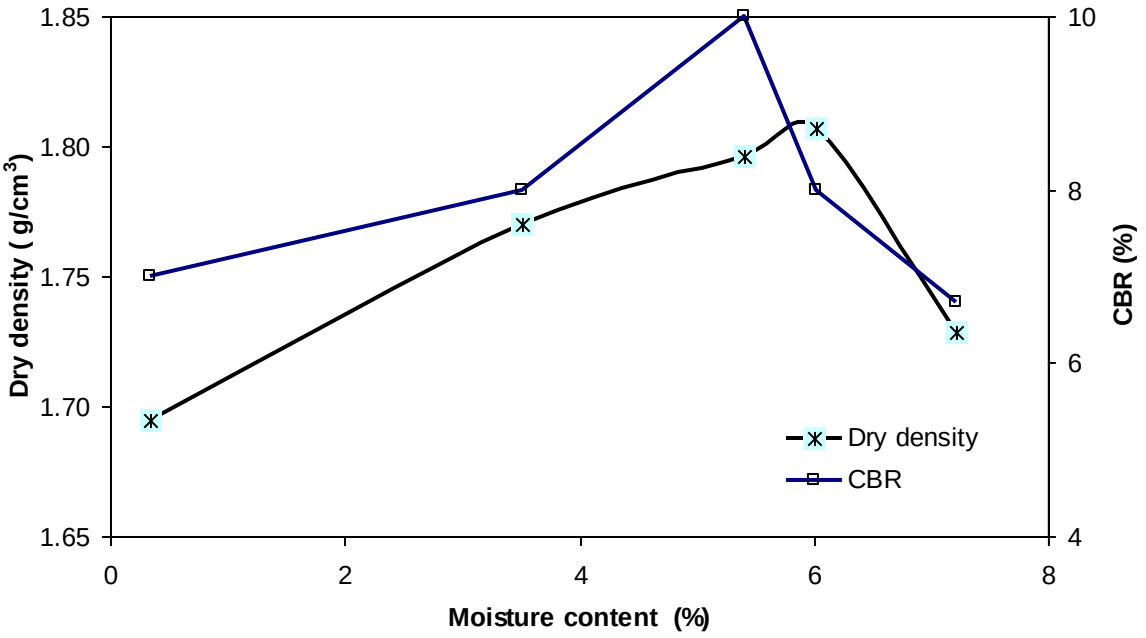

FIGURE 5 Compaction curve and CBR value of RAP.

MOVING WHEEL TEST RESULTS AND DISCUSSIONS

Test sections

The test pit was divided into four sections of equal area for the moving wheel test. The details of the four sections are shown in FIGURE 6. Section 1 was used as a control section for the test. The base course of Section 1 was 30-cm thick unreinforced AB-3 over the subgrade. Sections 2, 3, and 4 had 15-cm thick geocell-reinforced QW, RAP, and AB3, respectively. All the reinforced sections had a 2-cm thick cover of the respective materials on top of the 15-cm thick geocell-reinforced bases.

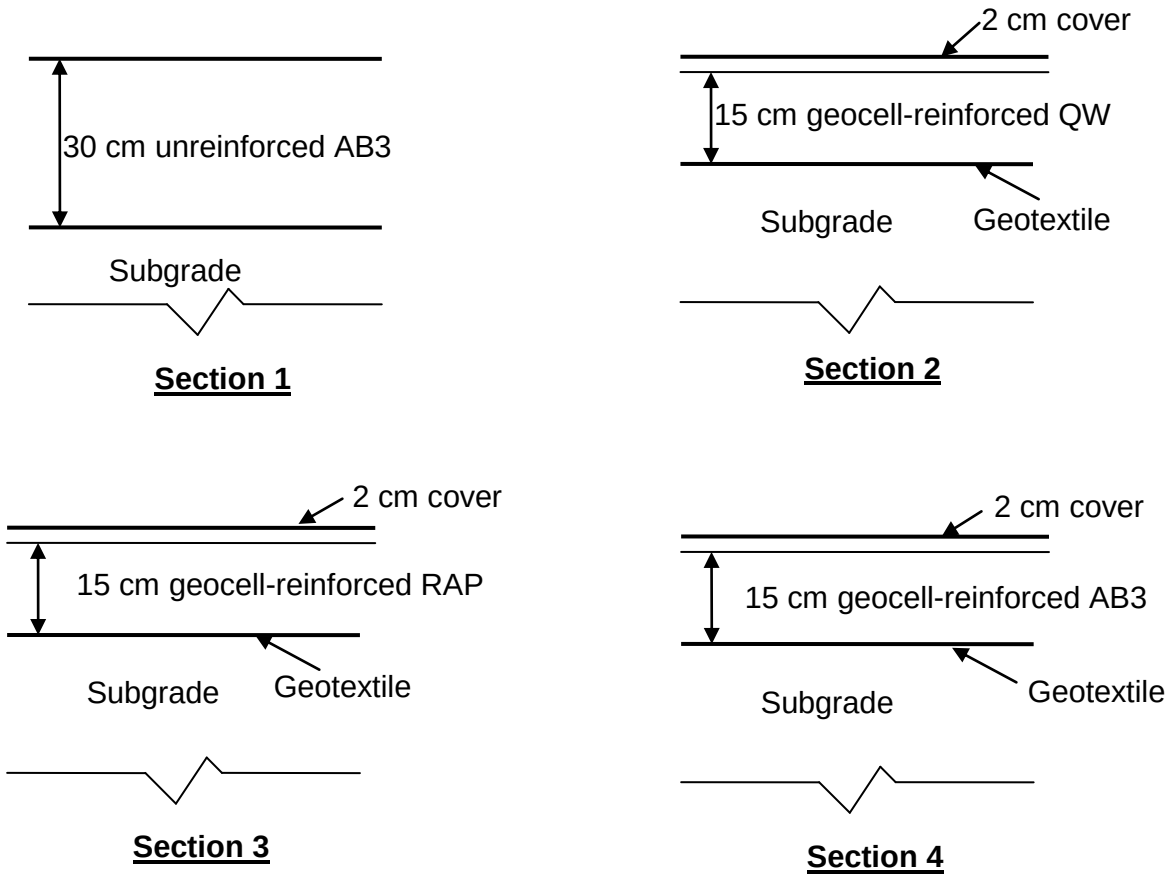

FIGURE 6 Test sections.

A vibratory compactor was used to compact the subgrade and base courses. The subgrade was prepared at 21% moisture content and compacted until a CBR value of about 3% was achieved. Vane shear, dynamic cone penetrometer (DCP), nuclear gauge, light falling weight deflectometer (LFWD), and falling weight deflectometer (FWD) tests were performed to evaluate the density and stiffness of the base courses. Sand cone tests were performed after the moving wheel test was completed.

Vane shear tests were carried out to ensure the subgrade CBR values during the preparation of subgrade. The percentage of CBR was estimated by the undrained shear strength (kPa) from the vane shear test divided by 30 kPa. This correlation was used by Giroud and Han (*3*) in their design method for geosynthetic-reinforced unpaved roads. The target CBR value was

3%. The average CBR values obtained from the vane shear tests on the ready-to-work subgrade were 2.5% at Section 1, 2.8% at Section 2, 3.4% at Section 3, and 2.7% at Section 4.

The desired density of the base courses was 95% of the maximum dry density. The compaction was performed on the wet side of the compaction curve within the range of 2% to the optimum moisture content. The control section was compacted in two lifts, i.e., 15 cm each lift while the reinforced sections were compacted in one lift. A nuclear gauge was used to monitor the level of compaction and density measurement during the compaction. DCP tests were carried out to estimate the CBR values of the test-ready sections (including the base and the subgrdae) using the Equation (1) (*15*):

$$CBR=292/(PI \times 25.4)^{1.12} \quad (1)$$

where PI = Penetration Index (in/blow) calculated based on the penetration per each blow. The DCP test results are plotted in FIGURE 7, which shows that the CBR value of the base course in Section 1 (the control section) was high compared to the other three reinforced sections.

Equal amount of compaction effort was applied to the base courses in all the four sections. The nuclear gage tests showed the final relative compaction before the test was 90% at Section 1, 98% at Section 2, 87% at Section 3, and 86% on Section 4. The sand cone tests after the moving wheel test found the compaction of 86% at Section 1, 93% at Section 2, 88% at Section 3, and 81% on Section 4. Although an equal compactive effort was applied in all the sections, DCP results showed that the average CBR value of the base course was 23% at Section 1 (the control section), 9% at Section 2, 7% at Section 3, and 10% at Section 4. In the control section, a CBR value of 47% was measured at a depth of about 25 cm from the surface. The control section therefore had the higher CBR values compared to those at the other three sections. FIGURE 7 also shows that the CBR values of the subgrade in all the sections were close to 3%. Due to the space limit, the test results of LFWD and FWD are not presented herein.

Rut depths

All four sections were subjected to the same moving wheel test. However, the rut depths in these sections developed at different rates. For example, the rut depth in the reinforced QW section (Section 2) increased rapidly within the first few passes and obvious heave around the wheel path was observed. At 50 passes, the measured rut depth was approximately 7 cm. The rut depth was measured from the peak and trough around the rut. It can be concluded that the QW at wet of the optimum moisture content was not strong enough to directly sustain the traffic loading. The moving wheel test was terminated at 305 passes because three of four sections reached more than 13-cm rut depth. Since the QW section has excessive rut depths, the QW and control sections were refilled during the test. Rut measurements on these two sections were not made after 205 passes. The rut data are plotted against the number of wheel passes for all four sections in FIGURE 8.

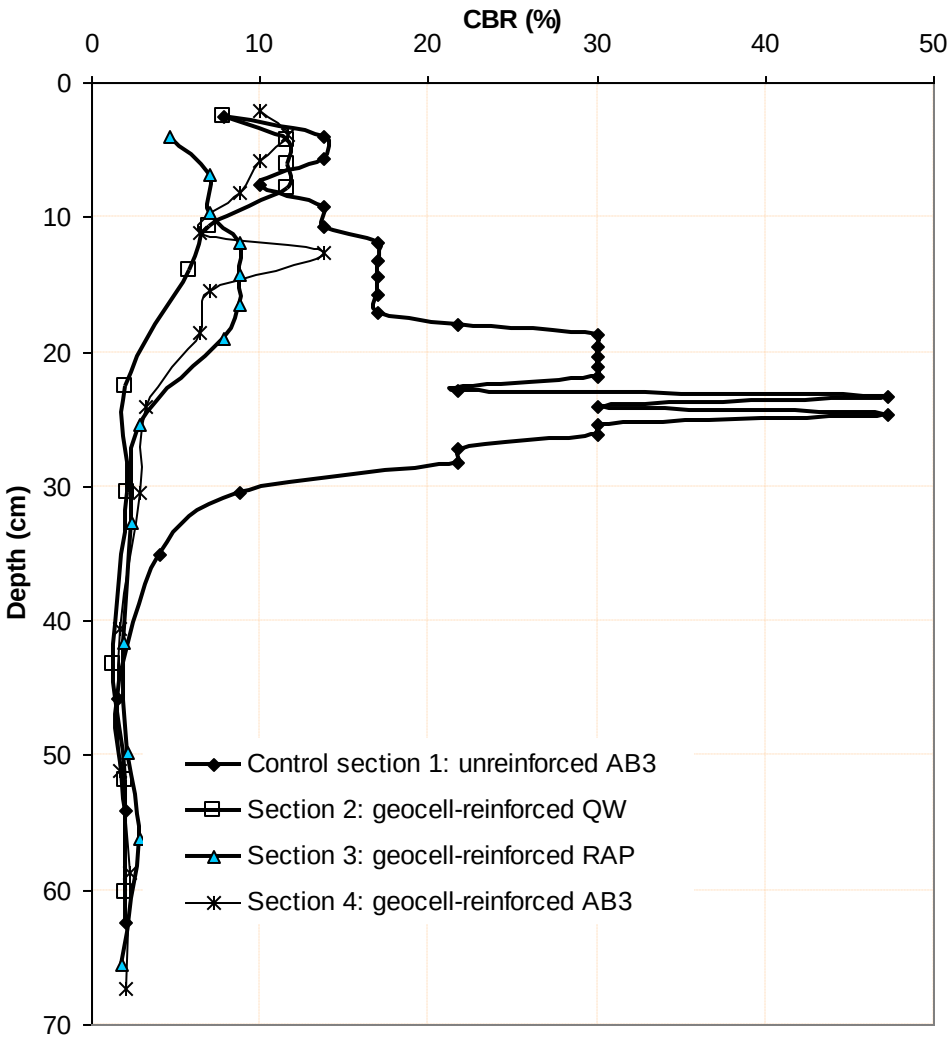

FIGURE 7 CBR from DCP tests.

FIGURE 8 shows that the reinforced QW section had the largest rut depth among all the test sections while the reinforced RAP section had the smallest rut depth. Even though the reinforced AB3 section had a thinner base thickness, it had a smaller rut depth than the unreinforced AB3 section. This result demonstrated that geocell reinforcement reduced the rut depth compared to the unreinforced section. The reinforced AB3 and RAP bases had the same thickness, however, the reinforced RAP base had a smaller rut depth than the reinforced AB3 especially at a larger number of passes. Visual observations showed that the reinforced RAP base was more stable than the reinforced AB3 base under the traffic loading.

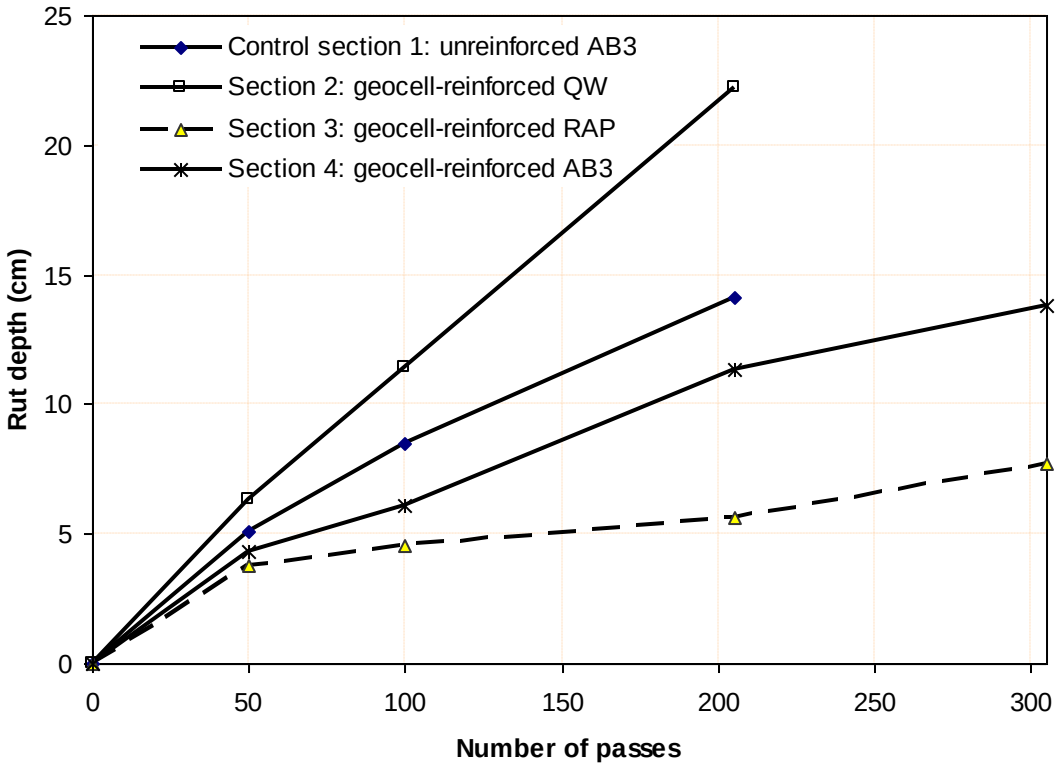

FIGURE 8 Rut depth versus number of passes.

Deformed profiles

After the moving wheel test, all the test sections were exhumed by trenches to examine the deformed profiles and geocells. In all the reinforced sections, geocells were initially laid out at 25 cm long in the traffic direction and 21 cm wide in the transverse direction. Forensic tests showed that the shape and size of the cells were intact outside the wheel path. However, under the wheel path, the average size was found to be 23.5 cm long in the traffic direction and 21.5 cm wide in the transverse direction. Some welds of the geocell in Sections 2 and 3 were broken at the edge of the wheel path. FIGURES 9-12 show the profiles of the test sections before and after the moving wheel test. The profiles are presented at the bottom (also the top of the subgrade) and top of the geocell for the reinforced sections but at the top of the subgrade for the unreinforced section. Due to the excessive rut and heave in Section 2 (the QW section), the exhumation of Sections 2 and 3 in the same path were conducted before re-filling (i.e., after 205 passes). Other two sections were exhumed after 305 passes. Patterns of rut and heave are clearly seen in all the sections. It is interestingly noticed that the rut depth and heave in each section were at the similar magnitude.

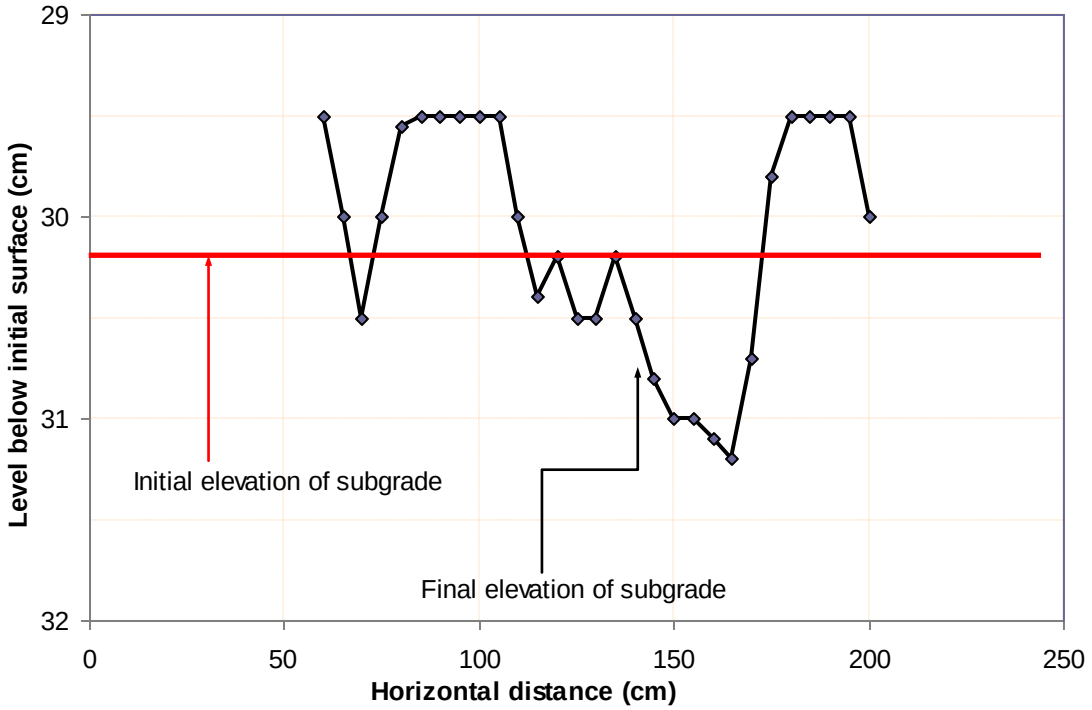

FIGURE 9 Control section 1- initial and final profiles after 305 passes.

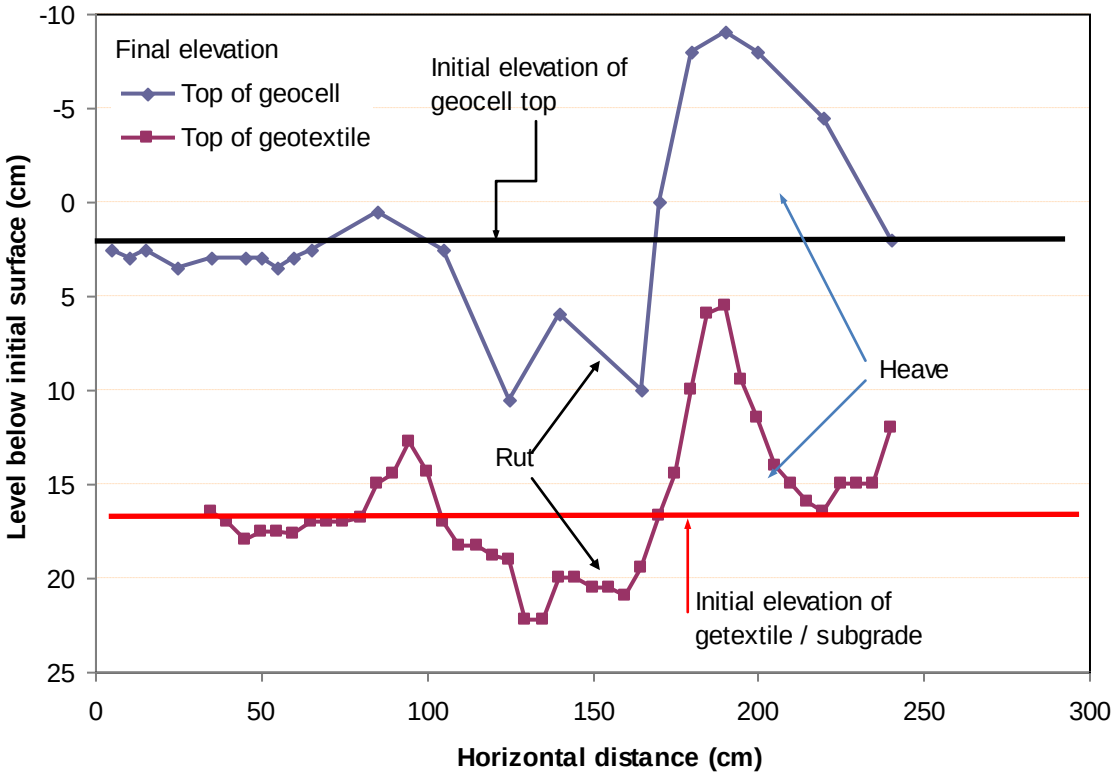

FIGURE 10 Reinforced QW section 2 - initial and final profiles after 205 passes.

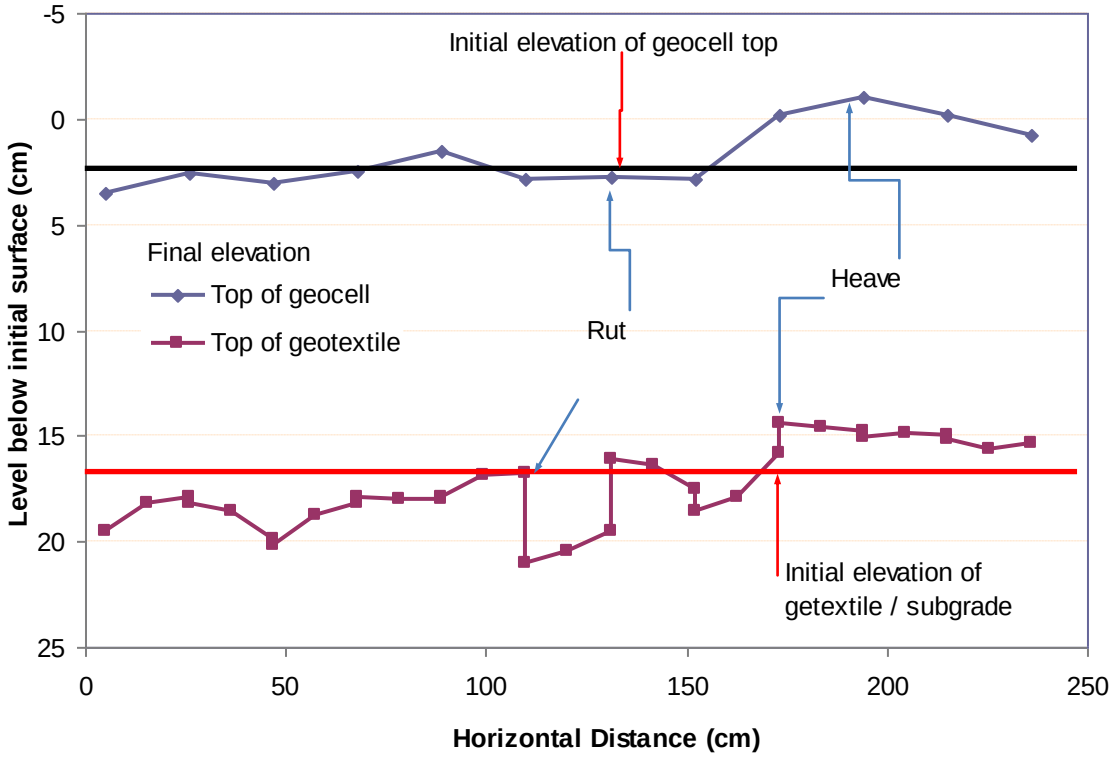

FIGURE 11 Reinforced RAP section 3 - initial and final profiles after 205 passes.

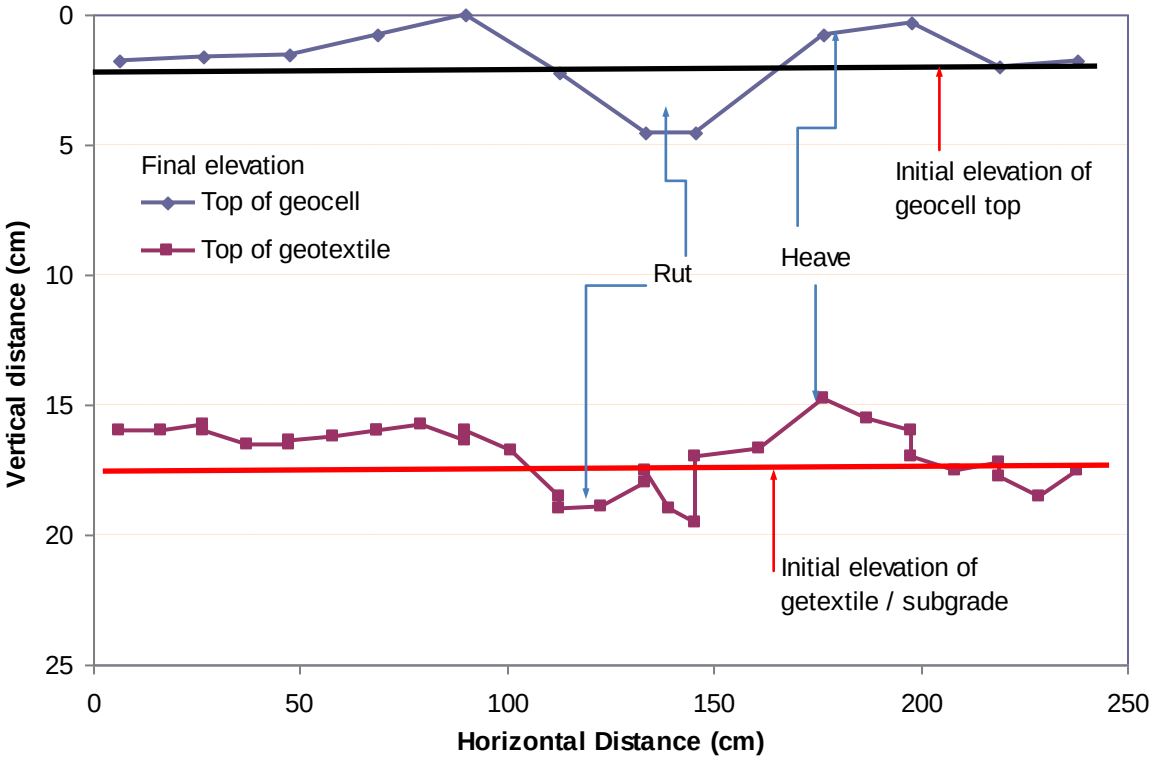

FIGURE 12 Reinforced AB3 section 4 - initial and final profiles after 305 passes.

Vertical stresses

Vertical stresses transmitted to the subgrade were measured by the pressure cells located at the subgrade-base interface. The measured vertical stresses are shown in FIGURE 13. It is shown that the measured vertical stresses were much lower than the tire pressure of 552 kPa applied on the road surface. FIGURE 13 also shows that the measured vertical stress increased with the number of passes, which is consistent with the design model proposed by Giroud and Han (*2*). Even though the control section had a base thickness of 30 cm compared to 17 cm in the reinforced AB3 section, their measured vertical stresses were close. This comparison demonstrates that geocell reinforcement reduced the vertical stress by distributing the load to a wide area. A stress distribution angle for each section can be calculated using the following formula:

$$p_i = \frac{P}{\pi(r + h\ tan\alpha)^2} \quad (2)$$

where p_i = the distributed vertical stress at the interface between the base course and the subgrade (kPa); P = the wheel load (kN); r = the radius of the tire contact area; h = the thickness of the base course; and α = the stress distribution angle. The distribution angles after 100 passes can be calculated from FIGURE 13 using Equation (2). The calculated stress distribution angles for the control section, the QW section, the RAP section, and the AB3 section were 29.2°, 35.7°, 40.8°, and 43.6°, respectively. Therefore, the reinforced AB3 section had the largest stress distribution angle among all the sections. Even though the reinforced QW section did not perform well, it had a higher stress distribution angle than that of the control section.

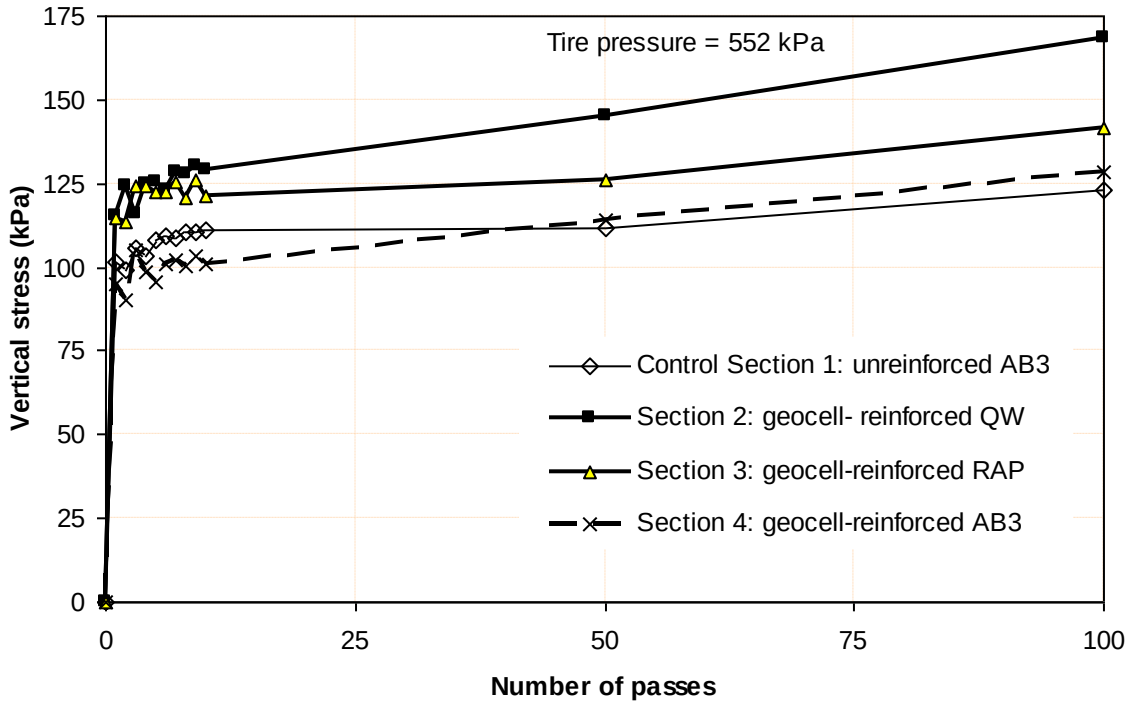

FIGURE 13 Measured vertical stresses at the subgrade-base interface.

Discussion

As discussed before, the geocell reinforcement can provide lateral confinement, beam effect, and wider stress distribution to the subgrade. These mechanisms ultimately contribute to the reduction of the base and subgrade deformations that result in a reduced rut depth at the surface. Based on the rut data in FIGURE 8, geocell reinforcement not only saved 13 cm of base material but also increased the life of the unpaved road as compared with the control section by 3.5 times for the reinforced RAP section and by 1.5 times for the reinforced AB3 section at the rut depth of 7.5 cm.

It is clearly evident from the results of the moving wheel test that geocell reinforcement of the base courses improved the strength and life of the unpaved sections except for the QW section. As the stress distribution angle was higher for the reinforced QW section, the initial failure was within the base course including the breakage of the welds. The failed weld connection rendered the geocell as a single unit rather than a monolithic honeycomb structure. It is also seen from FIGURE 3 that QW had more than 10% fines, which is sensitive to moisture. In other words, QW compacted at wet of optimum was too weak to hold the traffic loading. Due to the deterioration of the base course, the vertical stress increased rapidly as shown in FIGURE 13 and resulted in the failure of the subgrade.

Although the 17-cm reinforced AB3 and RAP sections showed the benefit over the 30-cm unreinforced AB3 control section, the benefit could have been more pronounced if a same level of compaction was achieved in all the sections. As shown in FIGURE 7, the control section had the highest CBR values among the four sections.

CONCLUSIONS

A full-scale, accelerated moving wheel test was conducted on four test sections, which included one control section with AB3 base course and three geocell-reinforced bases with AB3, quarry waste, and RAP as infill materials. The following conclusions can be drawn from this study:

1. 17-cm geocell-reinforced AB3 section had equivalent and even better performance than 30-cm AB3 control section even though the reinforced base was not that well compacted as the control base. The benefit could have been more pronounced if a same level of compaction had been achieved.
2. The geocell-reinforced RAP section performed better than the geocell-reinforced AB3 section with the same base thickness. However, the geocell-reinforced quarry waste section performed worse than the geocell-reinforced AB3 section. The quarry waste compacted at wet of the optimum moisture was too weak to sustain the traffic loading.
3. Geocell reinforcement increased the stress distribution angle by 13.4^{o} for the reinforced AB3 section, by 11.6^{o} for the reinforced RAP section, and by 6.5^{o} for the reinforced QW section, as compared with the control section.

ACKNOWLEDGMENTS

This research was jointly funded by the University of Kansas, Transportation Research Institute from Grant #DT0S59-06-G-00047, provided by the US Department of Transportation – Research

and Innovative Technology Administration and PRS Mediterranean, Inc. in Israel. This support is highly appreciated. The moving test was conducted at the APT facility of KSU. The authors would like to thank Prof. Mustaque Hossain, his students, Mr. Randy Testa (research technician) at KSU and the students and visiting scholars at the KU geotechnical group for their help during the section construction and testing.

REFERENCES

1. Tingle, J.S., and S.R. Jersey. Empirical Design Methods for Geosynthetic-Reinforced Low-Volume Roads. *Journal of the Transportation Research Board*. No. 1989. Vol. 2, 2007, pp. 91-101.
2. Giroud, J.P., and J. Han. Design Method for Geogrid-Reinforced Unpaved Roads. I. Development of Design Method. *ASCE Journal of Geotechnical and Geoenvironmental Engineering*, Vol. 130, No. 8, 2004, pp. 775-786.
3. Giroud, J.P., and J. Han. Design Method for Geogrid-Reinforced Unpaved Roads. II. Calibration of Applications. *ASCE Journal of Geotechnical and Geoenvironmental Engineering*, Vol. 130, No. 8, 2004, pp. 787-797.
4. Webster, S.L., Investigation of Beach Sand Trafficability Enhancement Using Sand-Grid Confinement and Membrane Reinforcement Concepts. *U.S. Army Engineer Waterways Experiment Station, Vicksburg, MS*, Report GL-79-20 (1), 1979.
5. Zhou, H., and X. Wen. Model Studies on Geogrid – or Geocell-Reinforced Sand Cushion on Soft Soil. *Geotextiles and Geomembranes*. 2007, Vol. 26, Issue 3, 2008, pp. 231-238.
6. Rajagopal, K., N.R., Krishnaswamy, and G.M. Latha. Behaviour of Sand Confined With Single and Multiple Geocells. *Geotextiles and Geomembranes*. Vol. 17, 1999, pp. 171 - 184.
7. Dash, S.K., K. Rajagopal, and N.R. Krishnaswamy. Performance of Different Geosynthetic Reinforcement Materials in Sand Foundations. *Geosynthetics International*, 11, No. 1, 2004, PP.35-42.
8. Wayne, M.H., Han, J., and Akins, K. The Design of Geosynthetic Reinforced Foundations. *Proceedings of ASCE's 1998 annual convention and Exposition*, Boston, Massachusetts, October 18-21, ASCE geotechnical special publication, No. 76, 1998, pp. 1-18.
9. Bathurst, R.J., and P.M. Jarrett. Large-scale model tests of geocomposite mattresses over peat subgrades. *Transportation Research Record 1188*, 1989, pp. 28-36.
10. Pokharel, S.K., J. Han, D. Leshchinsky, R.L. Parsons, and I. Halahmi. Experimental Evaluation of Influence Factors for Single Geocell-Reinforced Sand. *TRB 88th Annual Meeting, January 11 to 15, 2009*, Washington, DC.
11. Pokharel, S.K., J. Han, D. Leshchinsky, R.L. Parsons, and I. Halahmi. Behavior of Geocell-Reinforced Granular Bases under Static and Repeated Loads. *Contemporary topics in Ground Modification, Problem Soils, and Geo-Support, (Eds. Iskander, M., Laefer, D.F., and Hussein, M.H.), 2009 International Foundation Congress & Equipment*

Expo, March 15-19, 2009, Orlando, Florida. ASCE Geotechnical Special Publication 187, pp. 409-416.

12. Pokharel, S.K., J. Han, R.L. Parsons, Qian, Y., D. Leshchinsky, and I. Halahmi. Experimental Study on Bearing Capacity of Geocell-Reinforced Bases. *8th International Conference on Bearing Capacity of Roads, Railways and Airfields*, June 29 - July 2, 2009, Champaign, Illinois.
13. Pokharel, S.K., J. Han, D. Leshchinsky, R.L. Parsons, and I. Halahmi. Investigation of Factors Influencing Behavior of Single Geocell-reinforced Bases under Static Loading. Provisionally accepted for publication on *Journal of Geotextile and Geomembrane*. 2010.
14. Han, J., S.K. Pokharel, R.L. Parsons, D. Leshchinsky, and I. Halahmi. Effect of Infill Material on the Performance of Geocell-reinforced Bases. Accepted for presentation and publication at the *9th International Conference on Geosynthetics, ICG 2010*, May 23-27, 2010, Brazil.
15. Webster, S. L., R. H. Grau, and T. P Williams. Description and Application of Dual Mass Dynamic Cone Penetrometer. *Instruction Report GL-92-3*, 1992, Department of the Army, US Army Corp of Engineers, Washington, DC.

LIST OF FIGURE CAPTIONS